



СЕЙСМОСТОЙКОСТЬ СООРУЖЕНИЙ

SEISMIC RESISTANCE

DOI 10.22363/1815-5235-2022-18-2-161-171

UDC 699.841

RESEARCH ARTICLE / НАУЧНАЯ СТАТЬЯ

Macroseismic intensity-based catalogue of earthquakes in Ecuador

David Cajamarca-Zuniga^{1,2}, Oleg Kabantsev², Christopher Marin¹

¹Catholic University of Cuenca, Cuenca, Republic of Ecuador

²National Research Moscow State University of Civil Engineering, Moscow, Russian Federation

cajamarca.zuniga@gmail.com

Article history

Received: November 21, 2021

Revised: February 12, 2022

Accepted: February 29, 2022

Abstract. Earthquake magnitude catalogues and peak ground acceleration (PGA) maps for Ecuador may be found in several studies, however, there are rare works on the characterisation of the epicentral macroseismic intensities associated with earthquakes. In view of the concept that macroseismic intensity enables us to categorise the extent and severity of damage to buildings and structures caused by an earthquake, this study aims to compile a macro-seismic intensity-based catalogue of earthquakes in Ecuador, characterise the epicentral macroseismic intensities associated to seismogenic sources and perform a comparison with the National Seismic Hazard Map. This paper is the first that presents a catalogue of earthquakes with macroseismic intensities \geq VII and a series of maps of earthquake epicentres according to intensity, focal depth, data and magnitude of seismic events in Ecuador, based on the study of historical and instrumental records from 1900 to 2021. The obtained data shows that 95% of the territory of Ecuador has a PGA > 0.1 g, which corresponds to seismic intensities greater than VII, while regions with seismicity $>$ VIII ($ag = 0.2$ g) constitute 86%, and 3.8% of the territory of Ecuador has very high seismicity ($>$ IX), where the PGA exceeds 0.5 g. This information suggests that the normative National Seismic Hazard Map of Ecuador underestimate the hazard mainly in the south-east and in the Central Andes of Ecuador, and require an actualization.

Keywords: earthquake, Ecuador, macroseismic intensity, seismic hazard, seismicity, structural design

For citation

Cajamarca-Zuniga D., Kabantsev O., Marin C. Macroseismic intensity-based catalogue of earthquakes in Ecuador. *Structural Mechanics of Engineering Constructions and Buildings*. 2022;18(2):161–171.
<http://doi.org/10.22363/1815-5235-2022-18-2-161-171>

David Cajamarca-Zuniga, Docent of the Department of Civil Engineering, Catholic University of Cuenca, Ave Las Americas & Humboldt, Cuenca, 010101, Republic of Ecuador; PhD researcher, National Research Moscow State University of Civil Engineering, 26 Yaroslavskoye Shosse, Moscow, 129337, Russian Federation; ORCID: 0000-0001-8796-4635, Scopus ID: 57251506300, WoS ID: AAO-8887-2020, eLIBRARY SPIN-code: 6178-4383; cajamarca.zuniga@gmail.com

Oleg V. Kabantsev, Doctor of Technical Sciences, Professor, National Research Moscow State University of Civil Engineering, 26 Yaroslavskoye Shosse, Moscow, 129337, Russian Federation; ORCID: 0000-0001-9907-8470, Scopus ID: 15055871000, WoS ID: T-3937-2017, eLIBRARY SPIN-code: 2114-1185; ovk531@gmail.com

Christopher Marin, civil engineer, master student of the Department of Civil Engineering, Catholic University of Cuenca, Ave Las Americas & Humboldt, Cuenca, 010101, Republic of Ecuador; ORCID: 0000-0002-6601-032X; crmarin80@gmail.com

© Cajamarca-Zuniga D., Kabantsev O., Marin C., 2022

This work is licensed under a Creative Commons Attribution 4.0 International License
<https://creativecommons.org/licenses/by-nc/4.0/legalcode>

Каталог землетрясений Эквадора, основанный на макросейсмической интенсивности

Д. Кахамарка-Сунига^{1,2}  , О.В. Кабанцев²  , К. Марин¹ 

¹Католический университет города Куэнки, Куэнка, Республика Эквадор

²Национальный исследовательский Московский государственный строительный университет, Москва, Российская Федерация

 cajamarca.zuniga@gmail.com

История статьи

Поступила в редакцию: 21 ноября 2021 г.

Доработана: 12 февраля 2022 г.

Принята к публикации: 29 февраля 2022 г.

Для цитирования

Cajamarca-Zuniga D., Kabantsev O., Marin C. Macroseismic intensity-based catalogue of earthquakes in Ecuador // Строительная механика инженерных конструкций и сооружений. 2022. Т. 18. № 2. С. 161–171. <http://doi.org/10.22363/1815-5235-2022-18-2-161-171>

Аннотация. Каталоги магнитуд землетрясений и карты пиковых ускорений грунта (ПУГ, англ. PGA) для Республики Эквадор можно найти во многих исследованиях, однако работы, посвященные характеристике эпицентральной макросейсмической интенсивности, связанной с землетрясениями, встречаются редко. В связи с тем, что макросейсмическая интенсивность позволяет классифицировать степень и тяжесть ущерба, нанесенного землетрясением зданиям и сооружениям, целями данного исследования стали: 1) составление каталога землетрясений в Эквадоре на основе макросейсмической интенсивности; 2) характеристика эпицентральных макросейсмических интенсивностей, связанных с сейсмогенными источниками; 3) сравнение с Национальной картой сейсмической опасности. Впервые представлены каталог землетрясений с макросейсмической интенсивностью $\geq VII$ и серия карт эпицентров землетрясений в соответствии с интенсивностью, глубиной очага, данными и магнитудой сейсмических событий в Эквадоре, основанных на изучении исторических и инструментальных записей с 1900 по 2021 г. Полученные данные показывают, что 95 % территории Эквадора имеют $PGA > 0,1$ g, что соответствует сейсмической интенсивности более VII, регионы с сейсмичностью $> VIII$ ($ag = 0,2$ g) составляют 86 %, а 3,8 % территории Эквадора имеют очень высокую сейсмичность ($> IX$), где PGA превышает 0,5 g. Это свидетельствует о том, что нормативная Национальная карта сейсмической опасности Эквадора не учитывает опасность в основном на юго-востоке и в Центральных Андах Эквадора и требует актуализации.

Ключевые слова: землетрясение, Эквадор, макросейсмическая интенсивность, сейсмическая опасность, сейсмичность, сейсмостойкое проектирование

Introduction

The greatest earthquakes are known to occur at the tectonic plate interface of subduction zones. Ecuador is located at the northwest interface of the South American tectonic plate with the Nazca tectonic plate. This zone is part of the Rim of Fire, which is the world's most seismically active region. In this region about 90% of all earthquakes and about 80% of the strongest earthquakes have occurred¹ [1]. The Andes are one of the highest seismic activity regions in the world, accounting for around 20% of the Earth's total released seismic energy [2]. About 90% of continental territory of Ecuador presents high seismic hazard. The subduction of the Nazca tectonic plate and the complex system of active geological faults generates mostly shallow earthquakes in Ecuador, where the 7th world's largest earthquake was registered in 1906 ($Mw = 8.8$) [3; 4].

The definition of seismic hazard is fundamental to study the influence of the seismicity of a given region on earthquake-resistant structural design. In this work we present a catalogue of macroseismic events with intensities

Кахамарка-Сунига Давид, доцент департамента строительства, Католический университет города Куэнки, Республика Эквадор, 010101, Куэнка, Ave Las Americas & Humboldt; аспирант, Национальный исследовательский Московский государственный строительный университет, Российская Федерация, 129337, Москва, Ярославское шоссе, д. 26; ORCID: 0000-0001-8796-4635, Scopus ID: 57251506300, WoS ID: AAO-8887-2020, eLIBRARY SPIN-код: 6178-4383; cajamarca.zuniga@gmail.com

Кабанцев Олег Васильевич, доктор технических наук, профессор, Национальный исследовательский Московский государственный строительный университет, Российская Федерация, 129337, Москва, Ярославское шоссе, д. 26; ORCID: 0000-0001-9907-8470, Scopus ID: 15055871000, WoS ID: T-3937-2017, eLIBRARY SPIN-код: 2114-1185; ovk531@gmail.com

Марин Кристофер, инженер-строитель, магистр, Инженерный факультет, Католический университет города Куэнки, Республика Эквадор, 010101, Куэнка, Ave Las Americas & Humboldt; ORCID: 0000-0002-6601-032X; crmarin80@gmail.com

¹ United States Geological Survey. 20 Largest Earthquakes in the World. USGS. *Earthquake Hazards*. Available from: https://www.usgs.gov/natural-hazards/earthquake-hazards/science/20-largest-earthquakes-world?qt-science_center_objects=0#qt-science_center_objects (accessed: 20.02.2020).

greater than VII based on the study of seismogenic sources of Ecuador and its relation with the epicentres of historical high intensity earthquakes in order to compile a catalogue and maps of epicentres of earthquakes by intensities, years, depth and magnitudes, and compare the seismic events with the normative National Seismic Hazard Map of Ecuador.

To compile this catalogue, we reviewed pre-instrumental and instrumental information from several local, regional, and global sources such as IG-EPN, CERESIS, EHB, ISS, ISC, CENTENNIAL, NEIC, GCMT, USGS, and from other scientific works.

Based on the compiled catalogue, we have developed some maps of earthquakes locations according to registered intensities. In this paper, we also present the maps of epicentres of earthquakes by their intensities, years, depth and magnitudes, as well as comparison of the seismic events with both the normative National Seismic Hazard Map of Ecuador and the latest map of seismic hazard developed by the Ecuadorian Institute of Geophysics of the National Polytechnical School issued in 2021.²

Geodynamics of Ecuador and seismogenic sources

It is established that in the Equatorial latitudes the subducting process of the Nazca plate beneath the South American tectonic plate (55–75 mm/year) is the main and most evident geodynamic process in the north-western region of South America and in the territory of Ecuador (Figure 1) [5–8].

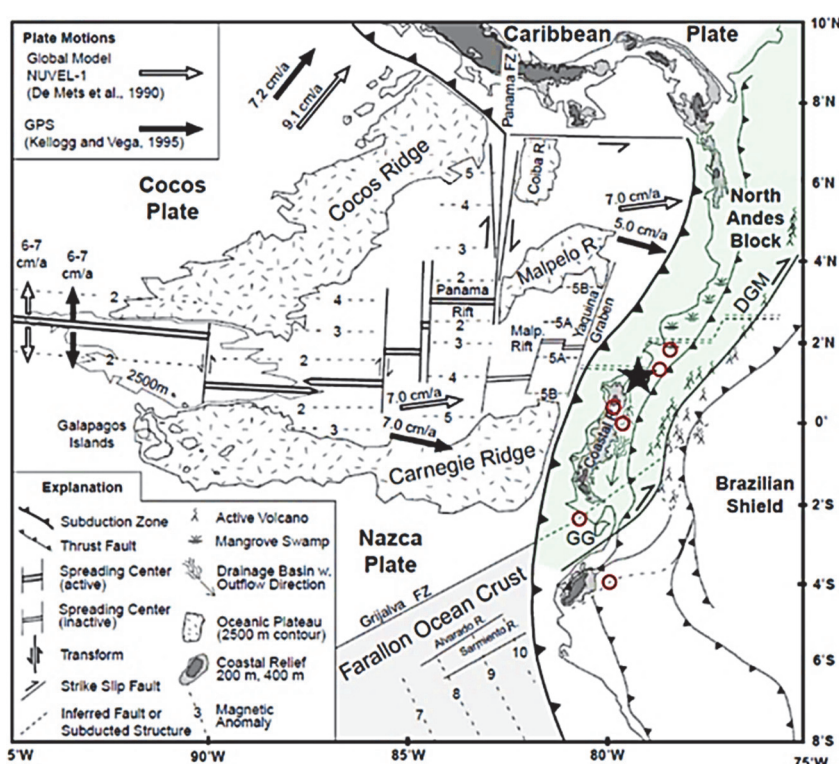


Figure 1. Tectonic setting, major faults and relative plate motions in Ecuador. Locations of the 1906 earthquake ($M_w = 8.8$, black star); from north to south the 1979, 1958, 2016, 1942, 1901, 1953 earthquakes ($M \geq 7.8$, red circles)

Source: edited after Gutscher et al., 1999 [7].

The segment of the Northern Andes where both thrust faulting and crustal shortening are observed coincides with the subduction zone of Carnegie Ridge. Along the subandean zone and the eastern cordillera of Ecuador, a large system of thrusts, as well as strike-slip and transpressive faults is located [9; 10]. Three main seismogenic sources affect the seismicity of Ecuador. The subduction of the oceanic Nazca plate beneath the continental South American plate is the major geodynamic process which controls the tectonic setting of this region and originates two other seismogenic sources: the subduction and collision of the Carnegie Ridge (CR), and the segmentation and “escape” of the North Andean Block (NAB) with an intricate strike-slip fault system [11]. The Ecuadorian Andes mainly defines a compression zone featured by reverse faults in the foothills essentially orthogonal to the plate convergence vectors and

² Catalogue of earthquakes in Ecuador. Mapa digital interactivo de peligro sísmico para Ecuador. Instituto Geofísico de la Escuela Politécnica Nacional (IG-EPN); 2021. Available from: <https://www.igepn.edu.ec/mapas/sismicidad/mapa-peligro-sismico> (accessed: 23.09.2021).

slip faults as the Dolores-Guayaquil Megashear (DGM) [12; 13] and the Chingual-Cosanga-Pallatanga-Puna (CCPP) fault system [8; 14], which are segments of the Guayaquil-Caracas Continental Megashear (GCM).

The subduction of the Carnegie Ridge controls the locations of large earthquakes and the clusterisation of seismic activity along the northwest coastline of Ecuador, as well as the evolution of the foothill basins of Borbon and Manabi, the uplifting of both the coast region and the Pastaza-Napo region at the Amazon basin [15–17]. The schematic geological cross-section of the subduction process at the collision zone of Carnegie Ridge between latitudes 1°N-2°S suggested in [18] shows geological events related to this process (Figure 2).

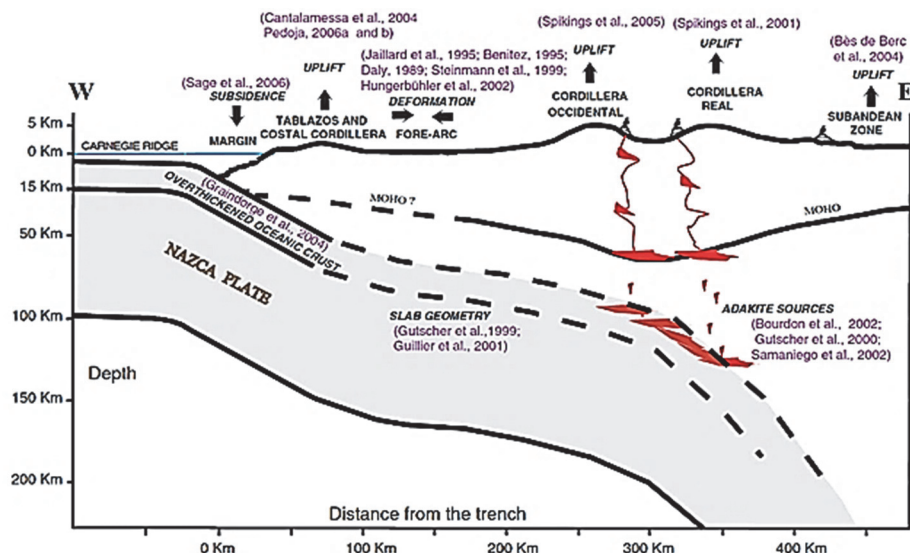


Figure 2. West-East cross-section of Ecuador at 1°11' S, showing geological events related to Carnegie Ridge subduction [18]

In the collision zone of the Carnegie Ridge, the orientation of crustal faults changes from north-south to northeast-southwest along the subduction margin [15; 19]. The morphology of the Ecuadorian subandean zone and

its strong tectonic activity can be attributed to a major geodynamic event, such as the subduction of Carnegie Ridge. The bulldozing effect associated to the subduction of the CR has contributed to uplift of the coastal ranges at rates of 0.30–0.50 mm/year for the Peninsula of Manta [20], and generates the northeastward displacement of the NAB along the Guayaquil-Caracas Continental Megashear [21].

To understand the geodynamic scheme of Ecuador, it is necessary to consider the movement of North Andean Block as a detaching “mini-plate” sliding through the northwest corner of South America on a large right-lateral strike-slip fault. This tectonic block is bordered on the north by the South Caribbean deformed belt, on the west by the Colombia-Ecuador trench and Panama Block, and on the east by the Guayaquil-Caracas Continental Megashear. As a result of this process the NAB is being ejected to the northeast following the front of the Eastern Cordillera along a transpressive system of faults [22–25]. According to recent studies [8; 23; 24; 26], the NAB is migrating relatively fast, just as the Nazca Plate is subducting to the east relative to the Amazonian Craton, the NAB is migrating to the north-east in relation to the South American plate at 6–10 mm/year. The Guayaquil Gulf opens at the southern junction between two fracture zones (the Colombia-Ecuador Trench and the GCM) that isolate the NAB [22]. The east Andean front fault zone starts east of the Gulf of Guayaquil as the dextral Pallatanga Fault [27–29]. Northern this fault continues as the Chingual-La

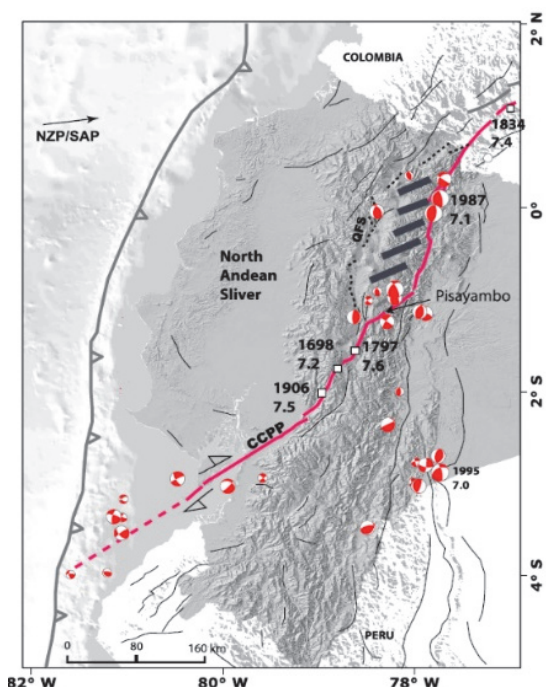


Figure 3. Chingual – Cosanga – Pallatanga – Puna (CCPP) fault system [8]

Columbia-Ecuador Trench and the GCM) that isolate the NAB [22]. The east Andean front fault zone starts east of the Gulf of Guayaquil as the dextral Pallatanga Fault [27–29]. Northern this fault continues as the Chingual-La

Sofia Fault [5; 8; 27; 28]. The motion of the North Andean Block “produces a complex system of active faults that generate shallow-focus earthquakes on the eastern front of the Andes” [21; 26].

The Chingual-Cosanga-Pallatanga-Puna fault system (Figure 3) is the most developed fault system in the territory of Ecuador and defines the NAB eastern tectonic border in Ecuador, where several shallow earthquakes have been registered [27]. The CCPP fault system extends from Guayaquil Gulf in Ecuador to the eastern “Cordillera Real” on the border between Ecuador and Colombia [8], then continues into Colombia as the Algeciras Fault [24]. It should be noted that multiple large earthquakes have occurred in the north-south trending segments of the CCPP fault and in the Carnegie Ridge collision zone. The shear zone of CCPP accounts for high cortical seismic activity in the central-northern Andes Cordillera of Ecuador.

Results and discussion

The main seismogenic source in Ecuador is the subducting process of the Nazca tectonic plate beneath the South American continental plate. In the background of this process, it is important to consider two factors: the influence of the Carnegie Ridge, which causes a “ploughing” effect (expression suggested by D. Cajamarca-Zuniga) on the shoreline and deep seismic activity in the Pastaza-Napo region at the Amazon basin, and the northward drift of North Andean block, which generates an intricate system of active strike-slip faults and generates shallow-focus earthquakes along the CCPP fault system.

The shoreline of Ecuador experienced large and great megathrust earthquakes along the northern flank of Carnegie Ridge collision zone: 1906 (Mw 8.8, intensity IX), 1942 (Mw 7.8, intensity IX), 1958 (Mw 7.7, intensity VIII), 1979 (Mw 8.2, intensity VIII), 2016 (Mw 7.8, intensity IX) [3; 30].

The central-north Andean region of Ecuador shows high crustal activity and registers multiple large historical earthquakes along the NNE-trending zone of CCPP fault system. Earthquakes with epicentral macroseismic intensity \geq VIII have occurred in 1541, 1557, 1575, 1587, 1645 (Mw 7, intensity IX), 1698 (Mw 7.7, intensity IX), 1755, 1757, 1797 (Mw 8.3, intensity XI), 1834, 1868 (Mw 7, intensity IX), 1923, 1926, 1938 (Mw 6.3, intensity VIII), 1949 (Mw 6.7, intensity X), 1996 (Mw 5.5, intensity VIII) [10; 31], mainly along NE-SW fault systems governed by the Guayaquil-Caracas Continental Megashear.

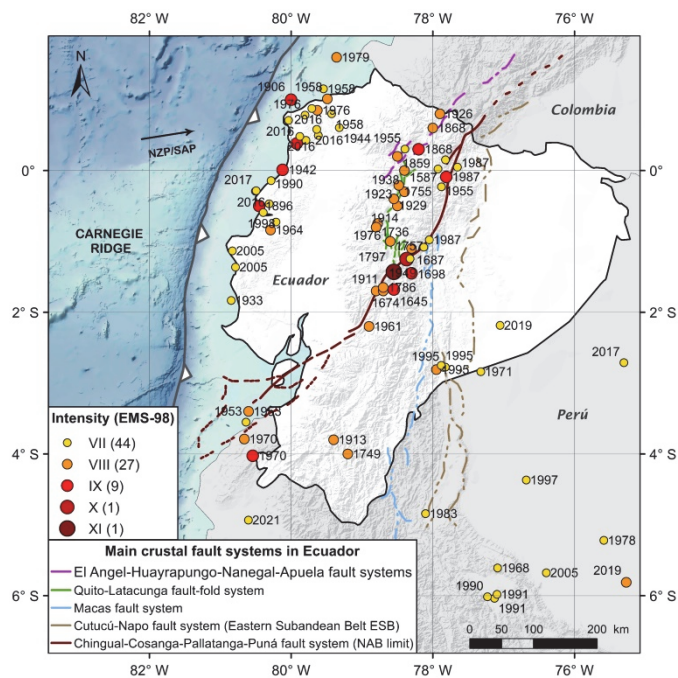


Figure 4. Location and years of earthquakes with macroseismic intensities \geq VII from 1900 to 2021. Here we can see the major seismic intensity at the collision zone of the subducting Carnegie Ridge (CR), as well as along the CCPP fault system

The sub-Andean zone at the Amazon basin shows an intermediate-depth seismicity in the Pastaza-Napo region and a high shallow-focus activity to the south, between the Macas and Quito-Napo fault systems: 1961 (Mw 6.6,

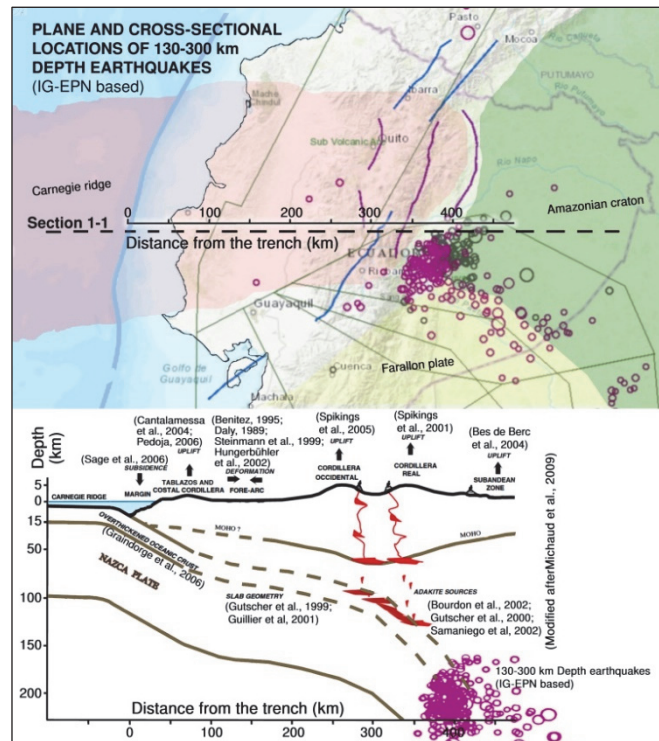


Figure 5. Plane and cross-sectional locations of 130–300 km depth earthquakes, that show the inferred 400 km prolongation of Carnegie Ridge beneath the territory of Ecuador

intensity VIII), 1971 (Mw 7.4, intensity VII), 1987 (Mw 6.4, intensity IX), 1995 (Mw 6.5, intensity VIII), 2019 (Mw 7.5, intensity VII)³ [32; 33].

In the Figure 4 we present a map developed in ArcMap software and show the epicentres and years of earthquakes with macroseismic intensities \geq VII from 1900 to 2021, where we can see the major seismic intensity at the Carnegie Ridge collision zone, as well as along the CCP fault system.

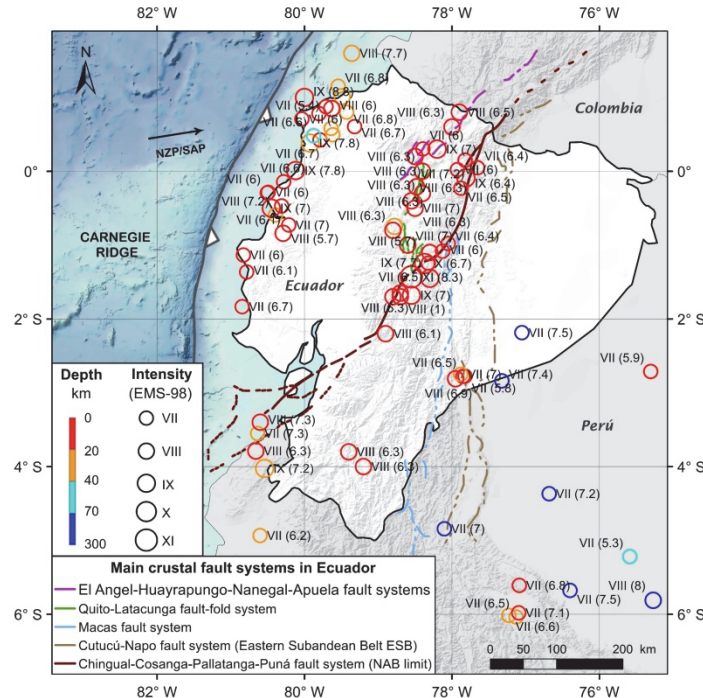


Figure 6. Locations and depth of earthquakes with intensities \geq VII from 1900 to 2021

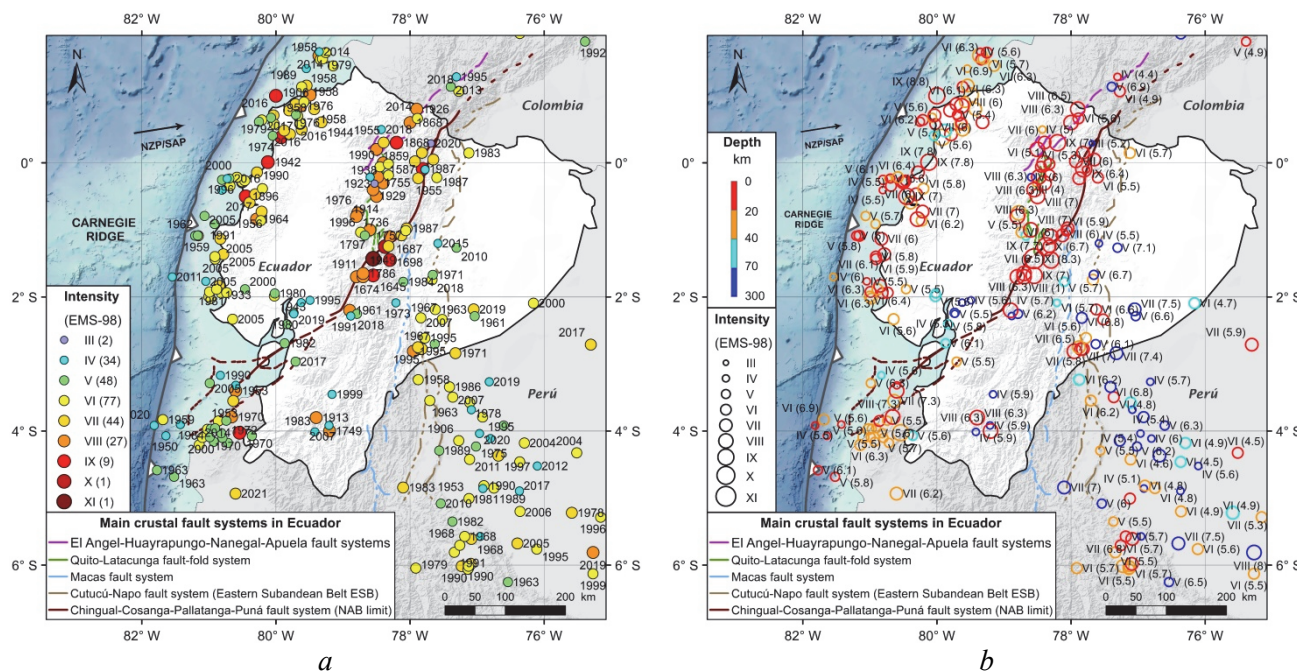


Figure 7. Location and years of earthquakes with intensities \geq III from 1900 to 2021 (a) and location, depth, intensity and magnitude of earthquakes with intensities \geq III from 1900 to 2021 (b)

³ United States Geological Survey. Earthquake catalog. *USGS. Earthquake Hazards program*. Available from: <https://earthquake.usgs.gov/earthquakes/search/> (accessed: 30.07.2021); *Catálogo Homogenizado 1587–2011. Sismicidad*. Instituto Geofísico de la Escuela Politécnica Nacional (IG-EPN). Available from: <https://igepn.edu.ec/mapas/sismicidad/mapa-catalogo-homogenizado> (accessed: 30.07.2021).

Catalogue of 1900–2021 Ecuador earthquakes with macroseismic intensities $\geq VII$

| Date, dd/mm/yyyy | Time, UTC | Intensity, MMI | Magnitude | Scale | Depth, km | Location | Latitude, ° | Longitude, ° |
|---------------------|--------------|-------------------|-----------|-------|--------------|---|----------------|-----------------|
| 1587 | | VIII | 6.3 | Mw | | 20 km NNE of Quito. Ecuador | 0.00 | -78.40 |
| 1645 | | IX | 7 | Mw | | 11 km E of Riobamba. Ecuador | -1.68 | -78.55 |
| 1674 | | VIII | 6.3 | Mw | | 17 km WbS of Riobamba. Ecuador | -1.70 | -78.80 |
| 1687 | | VIII | 6.3 | Mw | | 39 km ENE of Ambato. Ecuador | -1.10 | -78.30 |
| 1698 | | IX | 7.7 | Mw | | 15 km ESE of Banos. Ecuador | -1.45 | -78.30 |
| 1736 | | VIII | 6.3 | Mw | | 25 km WNW of Latacunga. Ecuador | -0.80 | -78.80 |
| 1749 | | VIII | 6.3 | Mw | | Loja, Loja. Ecuador | -4.00 | -79.20 |
| 1755 | | VIII | 6.3 | Mw | | Quito, Pichincha. Ecuador | -0.21 | -78.48 |
| 1757 | | VIII | 7 | Mw | | 7 km S of Latacunga. Ecuador | -1.00 | -78.60 |
| 1786 | | VIII | 6.3 | Mw | | 6 km WNW of Riobamba. Ecuador | -1.65 | -78.70 |
| 1797 | | XI | 8.3 | Mw | | 15 km WbS of Baños. Ecuador | -1.43 | -78.55 |
| 1859 | | VIII | 6.3 | Mw | | 26 km W of Otavalo. Ecuador | 0.20 | -78.50 |
| 1868 | | IX | 7 | Mw | | 10 km SW of Ibarra. Ecuador | 0.30 | -78.20 |
| 1868 | | VIII | 6.3 | Mw | | 7 km WSW of El Angel. Ecuador | 0.60 | -78.00 |
| 1896 | | IX | 7 | Mw | | 4 km S of Canoa. Ecuador | -0.50 | -80.45 |
| 31/01/1906 | 15:36:10 | IX | 8.8 | Mw | 20 | 22 km NW of Atacames. Ecuador | 1.00 | -80.00 |
| 1911 | | VIII | 1 | Mw | | 6 km WSW of Riobamba. Ecuador | -1.70 | -78.70 |
| 1913 | | VIII | 6.3 | Mw | | 31 km NW of Loja. Ecuador | -3.80 | -79.40 |
| 1914 | | VIII | 7 | Mw | | 30 km S of Quito. Ecuador | -0.50 | -78.50 |
| 1923 | | VIII | 6.3 | Mw | | 30 km S of Quito. Ecuador | -0.50 | -78.50 |
| 1926 | | VIII | 6.5 | Mw | | 20 km W of Tulcan. Ecuador | 0.80 | -77.90 |
| 1929 | | VIII | 6.3 | Mw | | 19 km SSW of Quito. Ecuador | -0.40 | -78.55 |
| 02/10/1933 | 15:29:27 | VII | 6.7 | Mw | 15 | 43 km N of Santa Elena. Ecuador | -1.83 | -80.85 |
| 1938 | | VIII | 6.3 | Mw | | 15 km SE of Quito. Ecuador | -0.30 | -78.40 |
| 14/05/1942 | 02:13:27 | IX | 7.8 | Mw | 20 | 10 km SW of Pedernales. Ecuador | 0.01 | -80.12 |
| 23/10/1944 | 23:40:09 | VII | 6.7 | Mw | 20 | 35 km NNE of Quininde. Ecuador | 0.61 | -79.32 |
| 05/08/1949 | 19:08:52 | X | 6.7 | Mw | 15 | 20 km NE of Baños. Ecuador | -1.25 | -78.32 |
| 12/12/1953 | 17:31:29 | VIII | 7.3 | Mw | 25 | 14 km NNE of Zorritos. Peru | -3.55 | -80.64 |
| 11/05/1955 | 11:04:04 | VII | 6.5 | Mw | 15 | 42 km SE of Cayambe. Ecuador | -0.23 | -77.88 |
| 20/07/1955 | 21:00:47 | VII | 6 | Mw | 15 | 14 km W of Cotacachi. Ecuador | 0.30 | -78.39 |
| 16/01/1956 | 23:37:45 | VII | 7 | Mw | 20 | 7 km NNE of Tosagua. Ecuador | -0.73 | -80.21 |
| 19/01/1958 | 14:07:28 | VIII | 7.6 | Mw | 27.5 | 19 km ENE of Esmeraldas. Ecuador | 1.01 | -79.49 |
| 19/01/1958 | 14:43:30 | VII | 6.8 | Mw | 27.5 | 23 km NE of Esmeraldas. Ecuador | 1.15 | -79.54 |
| 14/04/1958 | 21:32:34 | VII | 6.8 | Mw | 25 | 30 km SE of Esmeraldas. Ecuador | 0.80 | -79.43 |
| 28/07/1961 | 01:05:31 | VIII | 6.6 | Mw | 142.1 | 47 km E of Taisha. Ecuador | -2.29 | -77.04 |
| 19/05/1964 | 23:03:40 | VIII | 6.2 | Mw | 35 | 7 km WSW of Calceta. Ecuador | -0.86 | -80.23 |
| 09/02/1967 | 15:24:49 | IX | 7 | Mw | 55 | 162 km NNE of Florencia. Colombia | 2.85 | -74.80 |
| 19/06/1968 | 08:13:35 | VII | 6.8 | Mw | 15 | 49 km NNW of Moyobamba. Peru | -5.61 | -77.09 |
| 10/12/1970 | 04:34:41 | IX | 7.2 | Mw | 25 | 15 km SE of Cainaveral. Peru | -4.03 | -80.54 |
| 27/07/1971 | 02:02:49 | VII | 7.4 | Mw | 120 | 103 km ESE of Sucua. Ecuador | -2.84 | -77.32 |
| 02/10/1974 | 02:54:59 | VII | 5.7 | Mb | 5 | 48 km SW of Sechura. Peru | -5.91 | -81.09 |
| 09/04/1976 | 07:08:47 | VIII | 6.7 | Ms | 9 | 25 km SW of Esmeraldas. Ecuador | 0.78 | -79.80 |
| 06/10/1976 | 09:12:38 | VIII | 5.7 | Mb | 33 | 16 km NW of Saquisilí. Ecuador | -0.75 | -78.78 |
| 24/03/1978 | 12:31:22 | VII | 5.3 | Mb | 42 | 9 km E of Lagunas. Peru | -5.22 | -75.59 |
| 12/12/1979 | 07:59:03 | VIII | 7.7 | Ms | 24 | 68 km WNW of San Lorenzo. Ecuador | 1.60 | -79.36 |
| 31/03/1983 | 13:12:52 | VIII | 5.5 | Mb | 22.2 | 8 km WNW of Popayan. Colombia | 2.46 | -76.69 |
| 12/04/1983 | 12:07:54 | VII | 7 | Mw | 104.2 | 92 km NNE of La Peca. Peru | -4.84 | -78.10 |
| 22/11/1983 | 14:21:03 | VII | 6.6 | Mw | 54.9 | 21 km SE of Muisne. Ecuador | 0.48 | -79.88 |
| 25/12/1983 | 05:32:40 | VII | 5.4 | Mb | 33 | 49 km SSE of Saquena. Peru | -5.09 | -73.36 |
| 06/03/1987 | 08:14:48 | VII | 6 | Mw | 8.5 | 24 km E of Cayambe. Ecuador | 0.02 | -77.93 |
| 06/03/1987 | 01:54:50 | VII | 6.4 | Mw | 14.1 | 49 km SE of Pimampiro. Ecuador | 0.05 | -77.65 |
| 06/03/1987 | 04:10:41 | VII | 7.2 | Mw | 10 | 29 km SSE of Pimampiro. Ecuador | 0.15 | -77.82 |
| 22/09/1987 | 13:43:37 | IX | 6.4 | Mw | 10 | 26 km W of Tena. Ecuador | -0.98 | -78.05 |
| 22/09/1987 | 16:21:35 | VII | 6 | Mw | 10 | 36 km WSW of Tena. Ecuador | -1.08 | -78.13 |
| 30/05/1990 | 02:34:05 | VII | 6.6 | Mw | 24.2 | 28 km E of Moyobamba. Peru | -6.02 | -77.23 |
| 02/09/1990 | 04:26:48 | VII | 6.6 | Mw | 14.2 | 34 km SW of Pedernales. Ecuador | -0.14 | -80.28 |
| 04/04/1991 | 15:23:20 | VII | 6.5 | Mw | 20.7 | 4 km ENE of Rioja. Peru | -6.04 | -77.13 |
| 05/04/1991 | 04:19:49 | VII | 7.1 | Mw | 19.8 | 11 km NE of Rioja. Peru | -5.98 | -77.09 |
| 06/06/1994 | 20:47:40 | IX | 6.8 | Mw | 12.1 | 23 km E of Toribio. Colombia | 2.92 | -76.06 |
| 03/10/1995 | 12:44:58 | VIII | 6.5 | Mw | 16.7 | 50 km SE of Sucua. Ecuador | -2.78 | -77.85 |
| 03/10/1995 | 01:51:23 | VII | 7 | Mw | 24.4 | 45 km SE of Sucua. Ecuador | -2.75 | -77.88 |
| 07/10/1995 | 21:28:03 | VII | 5.8 | Mw | 12.3 | 52 km SE of Sucua. Ecuador | -2.78 | -77.82 |
| 25/08/1996 | 14:09:03 | VIII | 5.5 | Mwc | 50.7 | 10 km WSW of Salcedo. Ecuador | -1.08 | -78.67 |
| 28/10/1997 | 06:15:17 | VII | 7.2 | Mwc | 112 | 51 km N of Barranca. Peru | -4.37 | -76.68 |
| 04/08/1998 | 18:59:20 | VIII | 7.2 | Mwc | 33 | 3 km E of Bahía de Caraquez. Ecuador | -0.59 | -80.39 |
| 21/01/2005 | 13:45:14 | VII | 6 | Mwb | 10 | 21 km WSW of Montecristi. Ecuador | -1.13 | -80.83 |
| 24/01/2005 | 23:23:26 | VII | 6.1 | Mwb | 16.9 | 23 km W of Jipijapa. Ecuador | -1.36 | -80.79 |
| 26/09/2005 | 01:55:37 | VII | 7.5 | Mwb | 115 | 39 km NW of Yurimaguas. Peru | -5.68 | -76.40 |
| 16/04/2016 | 23:58:36 | IX | 7.8 | Mww | 20.59 | 27 km SSE of Muisne. Ecuador | 0.38 | -79.92 |
| 20/04/2016 | 08:35:10 | VII | 6 | Mwb | 10 | 10 km N of Muisne. Ecuador | 0.71 | -80.04 |
| 22/04/2016 | 03:03:41 | VII | 6 | Mww | 10 | 34 km NNW of Bahía de Caraquez. Ecuador | -0.29 | -80.50 |
| 18/05/2016 | 07:57:02 | VII | 6.7 | Mww | 16 | 32 km SE of Muisne. Ecuador | 0.43 | -79.79 |
| 18/05/2016 | 16:46:43 | VII | 6.9 | Mww | 29.95 | 24 km NW of Quininde. Ecuador | 0.49 | -79.62 |
| 11/07/2016 | 02:11:04 | VII | 6.3 | Mww | 21 | 33 km NNW of Quininde. Ecuador | 0.58 | -79.64 |
| 19/12/2016 | 07:11:39 | VII | 5.4 | Mwr | 10 | 11 km SSW of Esmeraldas. Ecuador | 0.88 | -79.71 |
| 18/04/2017 | 17:49:55 | VII | 5.9 | Mww | 14 | 151 km NE of Alianza Cristiana. Peru | -2.71 | -75.30 |
| 30/06/2017 | 22:29:45 | VII | 6 | Mww | 13 | 35 km NNW of Bahía de Caraquez. Ecuador | -0.28 | -80.49 |
| 03/12/2017 | 11:19:05 | VII | 6.1 | Mww | 17 | 18 km NE of Bahía de Caraquez. Ecuador | -0.47 | -80.31 |
| 22/02/2019 | 10:17:23 | VII | 7.5 | Mww | 145 | 115 km ESE of Palora. Ecuador | -2.19 | -77.05 |
| 26/05/2019 | 07:41:15 | VIII | 8 | Mww | 122.57 | 78 km NE of Navarro. Peru | -5.81 | -75.27 |
| 30/07/2021 | 17:10:19 | VII | 6.2 | Mww | 32.66 | 9 km ESE of Sullana. Peru | -4.93 | -80.60 |

The geodynamic and seismic activity in the territory of Ecuador suggest that the prolongation of the CR and the geological expression of its subduction beneath Ecuador requires about 400 km from the Colombia – Ecuador – Peru trench. In the Figure 5 we show the locations of depth earthquakes epicentres according to data from the IG-EPN earthquake catalogue.⁴ Also, we suppose that the eastern interface boundary of the Carnegie Ridge under the territory of Ecuador may be a triple junction of the Nazca tectonic plate with the Farallon plate and the Amazonian Craton, which probably controls the intermediate-depth seismicity in the Pastaza-Napo region at the Amazon basin.

Regarding the influence of earthquakes on buildings and structures, the only magnitude of an earthquake does not allow us to understand the level of damage to the structures, as it depends on other factors. For understanding the effects of an earthquake on buildings and structures, it is important to know and understand the macroseismic intensity of earthquakes. This concept enables us to categorise the extent and severity of earthquake-related damage to structures. Below we present information and maps related to earthquakes in Ecuador from 1900 to 2021 according to the intensity, focal depth and magnitude of each event. The proposed maps were developed in ArcMap software for geospatial data processing.

In the Figure 6 we show the epicentres and depth of earthquakes with intensities $\geq VII$ from 1900 to 2021. The Figure 7, a presents a map of earthquake epicentres with intensities $\geq III$ and the corresponding year of each event from the 1900 to 2021. In the Figure 7, b we present a map that shows the depth, intensities and magnitudes of earthquakes with intensities $\geq III$ from 1900 to 2021.

In the Table we present a catalogue of earthquakes with macroseismic intensities $\geq VII$ based on historical and instrumental records from 1900 to date⁵ [2; 5; 14; 31; 32].

We provide a comparison intensity-based map of earthquakes with both, the National Seismic Hazard Map of the Ecuadorian Building Standard NEC-SE-DS 2015 (Figure 8) and the latest (non-normative) probabilistic seismic hazard map issued by the Institute of Geophysics of the National Polytechnic School of Ecuador in 2021⁶ (Figure 9).

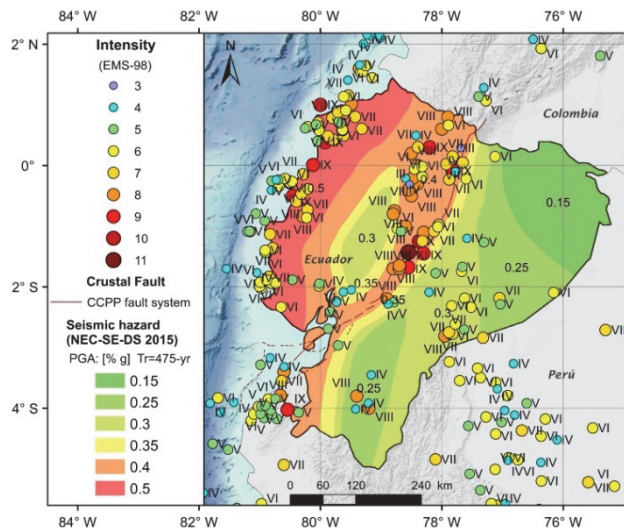


Figure 8. Comparison of earthquake epicentres by intensities $\geq III$ with the Normative seismic hazard map of Ecuador (NEC-SE-DS 2015)

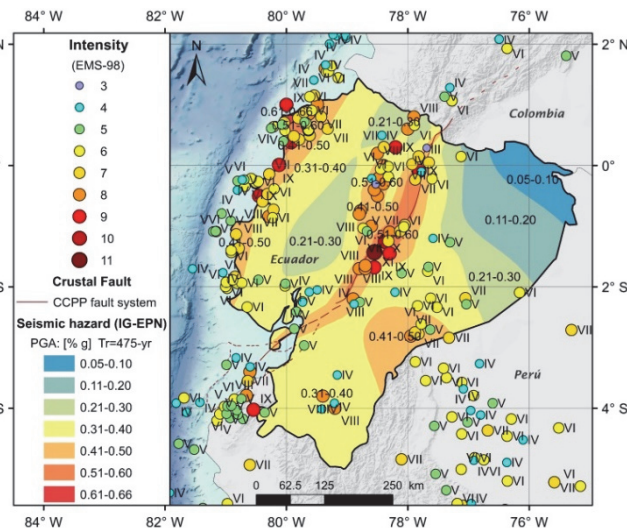


Figure 9. Comparison of earthquake epicentres by intensities $\geq III$ with the non-normative seismic hazard map issued by the Institute of Geophysics of the National Polytechnic School of Ecuador (IG-EPN, 2021)

⁴ Catalogue of earthquakes in Ecuador. *Mapa digital interactivo de peligro sísmico para Ecuador*. Instituto Geofísico de la Escuela Politécnica Nacional (IG-EPN); 2021. Available from: <https://www.igepn.edu.ec/mapas/sismicidad/mapa-peligro-sismico> (23.09.2021).

⁵ United States Geological Survey. 20 Largest Earthquakes in the World. *USGS. Earthquake Hazards*. Available from: https://www.usgs.gov/natural-hazards/earthquake-hazards/science/20-largest-earthquakes-world?qt-science_center_objects=0#qt-science_center_objects (accessed: 20.02.2020); *Catálogo Homogenizado 1587–2011. Sismicidad*. Instituto Geofísico de la Escuela Politécnica Nacional (IG-EPN). Available from: <https://igepn.edu.ec/mapas/sismicidad/mapa-catalogo-homogenizado> (accessed: 30.07.2021); *Catalogue of earthquakes in Ecuador. Mapa digital interactivo de peligro sísmico para Ecuador*. Instituto Geofísico de la Escuela Politécnica Nacional (IG-EPN); 2021. Available from: <https://www.igepn.edu.ec/mapas/sismicidad/mapa-peligro-sismico> (23.09.2021).

⁶ Catalogue of earthquakes in Ecuador. *Mapa digital interactivo de peligro sísmico para Ecuador*. Instituto Geofísico de la Escuela Politécnica Nacional (IG-EPN); 2021. Available from: <https://www.igepn.edu.ec/mapas/sismicidad/mapa-peligro-sismico> (23.09.2021).

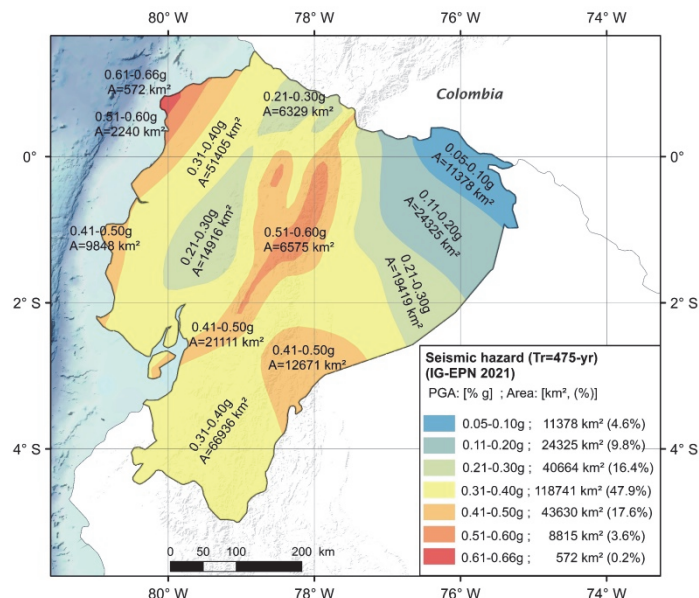


Figure 10. Areas of seismic regions, km², and their respective percentages in relation to the continental surface of Ecuador based on the non-normative seismic hazard map of the Institute of Geophysics of the National Polytechnic School of Ecuador (IG-EPN, 2021)

Based on the IG-EPN seismic hazard map for a return period of 475 years,⁷ we calculated the area of seismic regions and their respective percentages in relation to the continental surface of Ecuador, and prepared the map (Figure 10). The analysis of this map shows that 95% of the territory of Ecuador has a PGA > 0.1 g which corresponds to seismic intensities greater than VII [34–36], while regions with seismicity >VIII ($a_g = 0.2$ g) constitute 86%, and 3.8% of the territory of Ecuador has very high seismicity (>IX), where the peak seismic acceleration exceeds 0.5 g.

The analysis carried out in this research shows that the Normative Seismic Hazard Map of Ecuador underestimates the seismic hazard in the Central Andes and in the south-eastern region of the country. For instance, this paper shows that earthquakes up to X–XI intensity have been registered in the Central Andes of Ecuador, with an equivalent PGA above 0.5 g, while the Ecuadorian building standard (NEC-SE-DS 2015) specifies a PGA of 0.30–0.40 g for these zones.

Conclusion

Several scientific works present databases of magnitudes and maps of seismic activity in Ecuador, however, this paper is the first that provides a catalogue of earthquakes with macroseismic intensities greater than VII based on historical and instrumental records from 1900 to 2021. The studied events correspond to earthquakes of very strong and higher intensity levels, according to macroseismic scales MSK-64, MMI or EMS-98. Additionally, we have proposed a series of maps of earthquake epicentres according to intensity, focal depth and magnitudes that allow us to understand the actual effect of Ecuador's seismic activity on buildings and structures. The availability of this information in addition to the seismic hazard is relevant to study the influence of the seismicity of Ecuador on buildings and structures.

The main seismogenic sources in Ecuador are linked to the subduction process of the Nazca plate beneath the South American Plate. However, in this process, the convergence of the Carnegie Ridge, on one hand causes a ploughing effect resulting in shallow-focus earthquakes on the shoreline and deep seismic activity in the Pastaza-Napo region at the Amazon basin, and, on the other hand, the oblique collision of CR generates the northward drift of the NAB, which produces high seismic activity and shallow-focus earthquakes along the Central and Northern Andes.

The shoreline of Ecuador experienced large and great megathrust earthquakes mainly along the northern flank of Carnegie Ridge collision zone. The central and north Andean region of Ecuador shows high crustal activity and registers large historical earthquakes along the CCPP fault system. The sub-Andean zone at the Amazon basin shows an intermediate-depth seismicity in the Pastaza-Napo region and a high shallow-focus activity to the south, between the Macas and Quito-Napo fault systems.

⁷ Catalogue of earthquakes in Ecuador. Mapa digital interactivo de peligro sísmico para Ecuador. Instituto Geofísico de la Escuela Politécnica Nacional (IG-EPN); 2021. Available from: <https://www.igepn.edu.ec/mapas/sismicidad/mapa-peligro-sistmico> (23.09.2021).

The National Seismic Hazard Map of Ecuador underestimate the seismic hazard, mainly in the south-east of Ecuador and in the Central Andes region related to CCPP fault system, where events with macroseismic intensities up to X–XI (PGA > 0.5 g) have been registered. The obtained results suggest that the normative seismic hazard map of Ecuador deserves an actualization.

References

1. About earthquakes. In: Coffman J.L. (ed.) *Earthquake Information Bulletin* (vol. 3). Rockville: United States National Earthquake Information Center; 1971.
2. Giesecke A., Gómez Capera A.A., Leschiutta I., Migliorini E., Rodriguez Valverde L. The CERESIS earthquake catalogue and database of the Andean Region: background, characteristics and examples of use. *Annals of Geophysics*. 2004;47(2–3):421–435. <http://doi.org/10.4401/ag-3310>
3. Collot J.Y., Sanclemente E., Nocquet J.M., Leprêtre A., Ribodetti A., Jarrin P., Chlieh M., Graindorge D., Charvis Ph. Subducted oceanic relief locks the shallow megathrust in central Ecuador. *Journal of Geophysical Research: Solid Earth*. 2017;122(5):3286–3305. <http://doi.org/10.1002/2016JB013849>
4. Mayorga E.F., Sánchez J.J. Modelling of Coulomb stress changes during the great (Mw = 8.8) 1906 Colombia-Ecuador earthquake. *Journal of South American Earth Sciences*. 2016;70:268–278. <http://doi.org/10.1016/j.jsames.2016.05.009>
5. Beauval C., Marinière J., Yepes H., Audin L., Nocquet J.-M., Alvarado A., Baize S., Aguilar J., Singauch J.-C., Jomard H. A new seismic hazard model for Ecuador. *Bulletin of the Seismological Society of America*. 2018;108(3A):1443–1464. <http://doi.org/10.1785/0120170259>
6. Soto-Cordero L., Meltzer A., Bergman E., Hoskins M., Stachnik J.C., Agurto-Detzel H., Alvarado A., Beck S., Charvis Ph., Font Y., Hayes G.P., Hernandez S., Lynner C., Leon-Rios S., Nocquet J-M., Regnier M., Rietbrock A., Rolandone F., Ruiz M. Structural control on megathrust rupture and slip behavior: insights from the 2016 Mw 7.8 Pedernales Ecuador earthquake. *Journal of Geophysical Research: Solid Earth*. 2020;125(2). <http://doi.org/10.1029/2019JB018001>
7. Gutscher M.A., Malavieille J., Lallemand S., Collot J.Y. Tectonic segmentation of the North Andean margin: impact of the Carnegie Ridge collision. *Earth and Planetary Science Letters*. 1999;168(3–4):255–270. [http://doi.org/10.1016/S0012-821X\(99\)00060-6](http://doi.org/10.1016/S0012-821X(99)00060-6)
8. Alvarado A., Audin L., Nocquet J.M., Jaillard E., Mothes P., Jarrín P., Segovia M., Rolandone F., Cisneros D. Partitioning of oblique convergence in the Northern Andes subduction zone: migration history and the present-day boundary of the North Andean Sliver in Ecuador. *Tectonics*. 2016;35(5):1048–1065. <http://doi.org/10.1002/2016TC004117>
9. Fiorini E., Tibaldi A. Quaternary tectonics in the central Interandean Valley, Ecuador: fault-propagation folds, transfer faults and the Cotopaxi Volcano. *Global and Planetary Change*. 2012;90–91:87–103. <http://doi.org/10.1016/j.gloplacha.2011.06.002>
10. Tibaldi A., Rovida A., Corazzato C. Late Quaternary kinematics, slip-rate and segmentation of a major Cordillera-parallel transcurrent fault: the Cayambe-Afiladores-Sibundoy system, NW South America. *Journal of Structural Geology*. 2007;29(4):664–80. <http://doi.org/10.1016/j.jsg.2006.11.008>
11. Witt C., Bourgois J., Michaud F., Ordoñez M., Jiménez N., Sosson M. Development of the Gulf of Guayaquil (Ecuador) during the Quaternary as an effect of the North Andean block tectonic escape. *Tectonics*. 2006;25(3):1–22. <http://doi.org/10.1029/2004TC001723>
12. Baudino R., Hermoza W. Subduction consequences along the Andean margin: thermal and topographic signature of an ancient ridge subduction in the Marañón Basin of Perú. *Geologica Acta*. 2014;12(4):287–306. <http://doi.org/10.1344/GeologicaActa2014.12.4.2>
13. Kellogg J.N., Vega V., Stailings T.C., Aiken C.L.V. Tectonic development of Panama, Costa Rica, and the Colombian Andes: constraints from Global Positioning System geodetic studies and gravity. *Geologic and Tectonic Development of the Caribbean Plate Boundary in Southern Central America*. 1995;295:75–90. <http://doi.org/10.1130/SPE295-p75>
14. Dimate C., Drake L., Yepez H., Ocola L., Rendon H., Grunthal G., Giardini D. Seismic hazard assessment in the Northern Andes (PILOTO project). *Annali di Geofisica*. 1999;42(6):1039–1055. <http://doi.org/10.4401/ag-3787>
15. Hoskins M.C., Meltzer A., Font Y., Agurto-Detzel H., Vaca S., Rolandone F., Nocquet J-M., Soto-Cordero L., Stachnik J.C., Beck S., Lynner C., Ruiz M., Alvarado A., Hernandez S., Charvis Ph., Regnier M., Leon-Rios S., Rietbrock A. Triggered crustal earthquake swarm across subduction segment boundary after the 2016 Pedernales, Ecuador megathrust earthquake. *Earth and Planetary Science Letters*. 2021;553:116620. <http://doi.org/10.1016/j.epsl.2020.116620>
16. Pedroja K. *Les terrasses marines de la marge Nord Andine (Equateur et Nord Pérou): relations avec le contexte géodynamique*. Paris: Pierre and Marie Curie University (Paris 6); 2003.
17. De Berc S.B., Soula J.C., Baby P., Souris M., Christophoul F., Rosero J. Geomorphic evidence of active deformation and uplift in a modern continental wedge-top – Foredeep transition: example of the eastern Ecuadorian Andes. *Tectonophysics*. 2005;399(1–4 SPEC. ISS.):351–80. <http://doi.org/10.1016/j.tecto.2004.12.030>
18. Michaud F., Witt C., Royer J.Y. Influence of the subduction of the Carnegie volcanic ridge on Ecuadorian geology: reality and fiction. *Backbone of the Americas: Shallow Subduction, Plateau Uplift, and Ridge and Terrane Collision*. 2009;204:217–228. [http://doi.org/10.1130/2009.1204\(10\)](http://doi.org/10.1130/2009.1204(10))

19. Manchuel K., Régnier M., Béthoux N., Font Y., Sallarès V., Díaz J., Yepes H. New insights on the interseismic active deformation along the North Ecuadorian-South Colombian (NESC) margin. *Tectonics*. 2011;30(4):1–25. <http://doi.org/10.1029/2010TC002757>
20. Pedoja K., Dumont J.F., Lamothe M., Ortlieb L., Collot J.Y., Ghaleb B., Auclair M., Alvarez V., Labrousse B. Plio-Quaternary uplift of the Manta Peninsula and La Plata Island and the subduction of the Carnegie Ridge, central coast of Ecuador. *Journal of South American Earth Sciences*. 2006;22(1–2):1–21. <http://doi.org/10.1016/j.jsames.2006.08.003>
21. Staller A., Álvarez-Gómez J.A., Luna M.P., Béjar-Pizarro M., Gaspar-Escribano J.M., Martínez-Cuevas S. Crustal motion and deformation in Ecuador from cGNSS time series. *Journal of South American Earth Sciences*. 2018;86:94–109. <http://doi.org/10.1016/j.jsames.2018.05.014>
22. Dumont J.F., Santana E., Vilema W., Pedoja K., Ordóñez M., Cruz M., Jiménez N., Zambrano I. Morphological and microtectonic analysis of Quaternary deformation from Puná and Santa Clara Islands, Gulf of Guayaquil, Ecuador (South America). *Tectonophysics*. 2005;399(1–4 SPEC. ISS.):331–350. <http://doi.org/10.1016/j.tecto.2004.12.029>
23. Egbue O., Kellogg J. Pleistocene to present North Andean “escape.” *Tectonophysics*. 2010;489(1–4):248–257. <http://doi.org/10.1016/j.tecto.2010.04.021>
24. Yepes H., Audin L., Alvarado A., Beauval C., Aguilar J., Font Y., Cotton F. A new view for the geodynamics of Ecuador: implication in seismogenic source definition and seismic hazard assessment. *Tectonics*. 2016;35(5):1249–1279. <http://doi.org/10.1002/2015TC003941>
25. Taboada A., Rivera L.A., Fuenzalida A., Cisternas A., Philip H., Bijwaard H., Olaya J., Rivera C. Geodynamics of the northern Andes: subductions and intracontinental deformation (Colombia). *Tectonics*. 2000;19(5):787–813.
26. Nocquet J.M., Villegas-Lanza J.C., Chlieh M., Mothes P.A., Rolandone F., Jarrin P., Cisneros D., Alvarado A., Audin L., Bondoux F., Martin X., Font Y., Régnier M., Vallée M., Tran T., Beauval C., Maguiña Mendoza J.M., Martinez W., Tavera H., Yepes H. Motion of continental slivers and creeping subduction in the northern Andes. *Nature Geoscience*. 2014;7(4):287–291. <http://doi.org/10.1038/ngeo2099>
27. Ego F., Sébrier M., Lavenu A., Yepes H., Egues A. Quaternary state of stress in the Northern Andes and the restraining bend model for the Ecuadorian Andes. *Tectonophysics*. 1996;259(1–3 SPEC. ISS.):101–116. [http://doi.org/10.1016/0040-1951\(95\)00075-5](http://doi.org/10.1016/0040-1951(95)00075-5)
28. Soulas J.P., Eguez A., Yepes H., Perez H. Active tectonics and seismic hazard in the Ecuadorian Andes and the extreme south of Colombia. *Ecuadorian Geological Bulletin*. 1991;2(1):3–11.
29. Winter T., Avouac J.-P., Lavenu A. Late Quaternary kinematics of the Pallatanga strike-slip fault (Central Ecuador) from topographic measurements of displaced morphological features. *Geophysical Journal International*. 1993;115(3):905–920. <http://doi.org/10.1111/j.1365-246X.1993.tb01500.x>
30. Salocchi A.C., Minarelli L., Lugli S., Amoroso S., Rollins K.M., Fontana D. Liquefaction source layer for sand blows induced by the 2016 megathrust earthquake (Mw 7.8) in Ecuador (Boca de Briceño). *Journal of South American Earth Sciences*. 2020;103(June):102737. <http://doi.org/10.1016/j.jsames.2020.102737>
31. Beauval C., Yepes H., Palacios P., Segovia M., Alvarado A., Font Y., Aguilar J., Troncoso L., Sandro Vaca S. An earthquake catalog for seismic hazard assessment in Ecuador. *Bulletin of the Seismological Society of America*. 2013;103(2 A):773–786. <http://doi.org/10.1785/0120120270>
32. Beauval C., Yepes H., Bakun W.H., Egred J., Alvarado A., Singaudo JC. Locations and magnitudes of historical earthquakes in the Sierra of Ecuador (1587–1996). *Geophysical Journal International*. 2010;181(3):1613–1633. <http://doi.org/10.1111/j.1365-246X.2010.04569.x>
33. Swenson J.L., Beck S.L. Historical 1942 Ecuador and 1942 Peru subduction earthquakes, and earthquake cycles along Colombia-Ecuador and Peru subduction segments. *Pure and Applied Geophysics*. 1996;146:67–101. <http://doi.org/10.1007/bf00876670>
34. Richter C.F. *Elementary seismology* (J. Gilluly, A.O. Woodford, eds.). San Francisco: W.H. Freeman and Company; 1958.
35. Murphy J.R., O'Brien L.J. The correlation of peak ground acceleration amplitude with seismic intensity and other physical parameters. *Bulletin of the Seismological Society of America*. 1977;67(3):877–915. <http://doi.org/10.1785/BSSA0670030877>
36. Linkimer L. Relationship between peak ground acceleration and modified Mercalli intensity in Costa Rica. *Revista Geológica de América Central*. 2008;38:81–94.